

Side-Lobe Suppression for the Third Harmonic Resonance of Planar Dipole Antennas Using High Refractive Index Metamaterials

Xiao-Fei Zhang^{*}, Guang-Ming Wang, and Jian-Gang Liang

Abstract—In this paper, a simple and effective side-lobe suppression technique is proposed by using integrated high refractive index metamaterial (HRIM). It is known that current reversal, which occurs at the third harmonic of the dipole natural frequency, disturbs the omnidirectional radiation pattern of a dipole antenna, and the main beam splits into two side lobes. For suppressing the two side lobes and maintaining consistent radiation pattern purposes, two regions of HRIMs are integrated along the side-lobe radiation direction of a reflector-backed dipole antenna to tilt the two side lobes toward the broadside radiation direction. The HRIM is constructed with 2×3 H-shaped unit-cells periodically printed on the single side of dielectric substrates. The beam-tilting approach described here uses the phenomenon that the EM wave undergoes a phase shift when entering a medium of different refractive indices. Simulation and measurement results show that by implementing the HRIMs, the two side lobes are tilted toward the broadside radiation direction, and as a result, the side lobe is suppressed, and radiation consistency for the first and third harmonic resonances is realized. Moreover, the antenna gain for the third harmonic is achieved as high as 7.8 dBi, which is an increase of approximately 3 dBi compared with the fundamental resonance.

1. INTRODUCTION

With the rapid development of modern wireless communication systems, dipole antennas with low profile, light weight, and omnidirectional radiation patterns have been applied to a variety of applications such as wireless local area networks (WLANs), radio broadcasting, base stations, and satellite communication. It is well known that a conventional dipole antenna only resonates at the frequencies where the physical length of the dipole is an odd multiple of a half wavelength, which means that the dipole antenna resonates at harmonics of the fundamental resonances [1]. Moreover, the direction of the current on the dipole antenna flips every half wavelength, and the radiation field generated by the reverse current does not reinforce those generated by original current. As a result, the main beam splits, and the omnidirectional radiation patterns are disturbed. In practical wireless communication systems, to avoid radiated field deteriorating and obtain an omnidirectional radiation pattern, the physical length of a dipole antenna has to be less than a wavelength, and the dipole antenna is capacitive or resistively loaded. Nevertheless, the antenna directivity and radiation efficiency are relatively low compared with higher order harmonics due to the short electrical size [2]. Therefore, the design of a higher order harmonic resonance dipole antenna with an omnidirectional radiation pattern shows progress in antenna gain and radiation efficiency.

In recent years, metamaterials (MTM) which display exotic properties such as high refractive index (HRI) [3, 4], negative permittivity and permeability [5], have provided novel conceptual routes to design novel compact and high gain antennas [6]. In [7], an artificial magnetic conductor (AMC) is constructed with periodically placed capacitively loaded loops (CLL). By partly covering a monopole antenna with

Received 29 May 2019, Accepted 29 July 2019, Scheduled 20 August 2019

^{*} Corresponding author: Xiao-Fei Zhang (zxf1990fei@163.com).

The authors are with the Air and Missile Defense College, Air force Engineering University, Xi'an, Shaanxi 710051, China.

the AMC shell, the equivalent current distribution is improved, and omnidirectional radiation pattern is observed at the third harmonic of the main resonant frequency. However, the AMC cover is bulky in size, and the main beam still splits into two side lobes at higher frequencies. In [8], an artificial mu-negative transmission line (MNG-TL) structure is utilized to realize a wideband dipole antenna with stable radiation patterns. However, the resonant mode of the antenna is the MNG-TL resonant mode, which means that the antenna radiation pattern still deteriorates at higher order resonances, and the antenna directivity has not been improved. In [9], high refractive index metamaterial (HRIM) was implemented onto a planar bow-tie antenna to redirect the radiation beam, and the proposed beam tilting technique was focused on the fundamental resonant mode and shows no degradation of antenna gain, which is an improvement.

In this paper, side-lobe suppression is realized successfully for the third harmonic resonance of planar dipole antennas by using integrated HRIM. By implementing two regions of HRIMs along the side-lobe radiation direction of the reflector-backed dipole antenna, the two side lobes are tilted toward the broadside radiation direction. As a result, radiation consistency is realized, and the antenna gain is improved by 3 dBi.

2. SIDE-LOBE SUPPRESSION MECHANISM

The mechanism of side-lobe suppression by using HRIM is analyzed and elaborated in detail in this section. To make a clear insight into the side-lobe suppression technique, the beam-tilting approach is firstly discussed.

2.1. Beam Tilting Mechanism

In Fig. 1(a), an electromagnetic (EM) point source is placed in the vicinity of a two-sectioned medium with different refractive indexes. The EM wave that exits in each layer undergoes a different phase shift, which is given by:

$$\beta_1 = k_0 n_1 d \quad (1)$$

$$\beta_2 = k_0 n_2 d \quad (2)$$

The phase shift of β between the radiated EM wave is given by:

$$\beta = k_0(n_1 - n_2)d \quad (3)$$

Due to the existence of the phase shift of the emanating EM wave, the beam direction is tilted toward the high refractive index direction. The relation between β and tilting angle φ is expressed as:

$$\beta = k_0 l \sin \varphi \quad (4)$$

Therefore, by Eqs. (3) and (4), the tilting angle can be expressed as:

$$\varphi = \sin^{-1} \left[\frac{d(n_2 - n_1)}{l} \right] \quad (5)$$

According to Eq. (5), when the EM wave illuminates a medium of different refractive indexes, the beam will be tilted toward the region with higher refractive index, and the tilting angle is determined by dimensions of the medium and difference of the refractive index.

2.2. Side Lobe Suppression for the Third Harmonic

Generally speaking, for a conventional planar dipole antenna backed by a metal reflector, two side lobes besides the main beam will appear at the third harmonic resonance because of the current reversal on separate dipole arms. Under this circumstance, the radiation pattern is shaped in the form with a main beam and two side lobes, show in Fig. 1(b). When conventional material (CM), i.e., the dielectric substrate, is adopted in front of the EM source, the radiation pattern will stay unchanged.

To suppress the two side lobes for the third harmonic, two additional HRIMs are implemented along the side-lobe radiation direction in the vicinity of EM source as shown in Fig. 1(c). Here, one

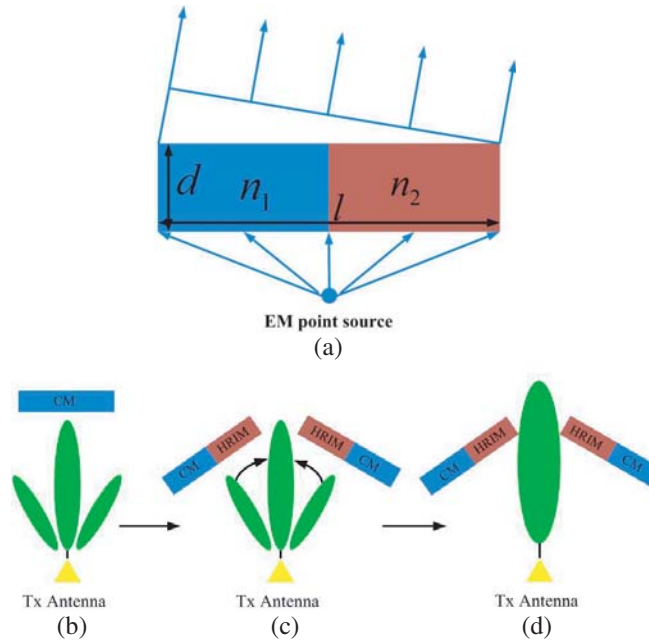


Figure 1. Illustration of beam tilting mechanism. (a) EM point source radiating toward materials with different refractive index. (b). Without HRIM loading, radiation pattern with two side lobes. (c). With HRIM loading, two side lobes are tilted toward the broadside radiation direction. (d) Radiated beams with enhanced gain.

point should be noted that the HRIM is sensitive to the illumination direction of EM source, and the high refractive index can be finely excited when the HRIM is perpendicular to the incident direction of the electromagnetic waves. Consequently, the HRIM region is designed with a tilting angle compared with the broadside direction. Based on the aforementioned beam tilting conclusion, the beam will be tilted toward the region with higher refractive index. With the aim of suppressing the two side lobes, two regions of HRIM are implemented in the broadside direction next to the CM. In this case, the two side lobes will be tilted toward the HRIM direction, i.e., the broadside radiation direction. At the same time, the main beam will remain in the broadside direction and stay unaffected because the incident direction of the main beam is oblique to the HRIM.

Moreover, the finely designed HRIM is sensitive to frequency, and the HRIM displays different refractive indexes as frequency increases. The aim of designing the HRIM is to realize a higher refractive index for the third harmonic resonance of the dipole antenna. By designing the HRIM properly for the third harmonic resonance of the dipole antenna and implementing it in vicinity of the dipole antenna, the two side lobes can be tilted toward the broadside direction, and the main beam stays unchanged. As a result, the finalized radiation pattern for the dipole antenna is one main beam without side lobes, which is shown in Fig. 1(d), and the aim of suppressing the side lobes for the third harmonic resonance is realized. In addition, as more electromagnetic energy is concentrated toward the broadside direction, the directivity for the third harmonic is increased compared the situation when there is no HRIM loading.

3. ANTENNA DESIGN WITH HRIM

The perspective view of the proposed antenna is illustrated in Fig. 2. The green and blue parts denote the metals on top and bottom of the dielectric substrate, respectively. The driven antenna is a reflector-backed dipole antenna to ensure that the radiation pattern is unidirectional. Two arrays of 2×3 H-shaped electric resonator are capacitively coupled to the driven dipole as parasitic HRIM elements. The overall size of the antenna is $40 \text{ mm} \times 60 \text{ mm}$, and the antenna is printed on an FR4 substrate with dielectric constant of 4.3, loss tangent of 0.002, height of 0.8 mm. The detailed dimensions of the

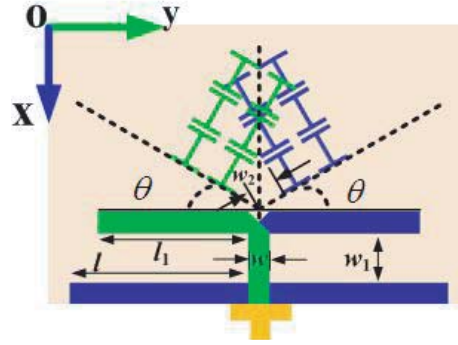


Figure 2. Perspective view of the proposed antenna

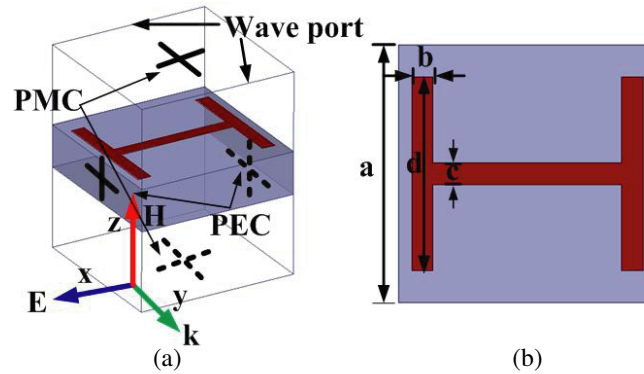


Figure 3. Simulation set up for the unit cell. (a) Port and excitation set up. (b) Detailed dimension of the unit cell.

antenna are: $l = 25$ mm, $w = 3$ mm, $l_1 = 21$ mm, $w_1 = 7$ mm, $\theta = 30^\circ$, $w_2 = 3.6$ mm. During the simulation process, the EM software, High Frequency Structure Simulator (HFSS) version 13.0, is used for full wave analysis of the antenna.

For a traditional half wave length dipole antenna, the main beam splits into two side lobes at the third harmonic resonance, and the side lobe is tilted by approximate 60° away from the broadside direction. To effectively excite the electric resonances of the HRIM, the incident direction of the electromagnetic wave has to be normal, and thus θ is carefully chosen to be 30° in the antenna design. Moreover, the gap w_2 between the EM point source and the HRIM plays a key role in determining the coupling capacitance. When w_2 increases, the coupling capacitance gets weak, and the HRIM will not be excited. When w_2 decreases, part of the HRIM is overlapped in the broadside direction, and the electric resonances will not stay the same. The optimized w_2 is chosen to be 3.6 mm. Under this circumstance, the overlapped part is relatively small in the broadside direction, and the coupling capacitance is strong.

The proposed HRI unit-cell structure, shown in Fig. 3(a), is a traditional H-shaped electric resonator. The unit-cell is simulated with PEC and PMC boundary conditions applied to yo z and xoy planes, respectively, and the two ports are located in Y-direction. The goal of designing the HRIM is to suppress the side lobe for the third harmonic resonance of the dipole which appears at around 7.2 GHz, so during the process in designing the HRIM, parameters of the HRIM should be finely tuned to make sure that the high refractive index is obtained at around 7.2 GHz. The detailed dimensions of the unit cell are: $a = 6$ mm, $b = 0.2$ mm, $c = 0.2$ mm, $d = 4.5$ mm. S parameters of the unit-cell structure are simulated, and its characterizing parameters are extracted using the algorithm described in [10].

The simulated S parameters of the unit cell are shown in Fig. 4(a). We can see that two electric resonances appear at 6.8 GHz and 9.2 GHz, respectively, and the magnetic resonance appears at 7.9 GHz. When the HRIM is working at the magnetic resonant frequency, S_{21} is so small that little energy can be transmitted through the substrate with the HRIM. In this paper, the third harmonic resonance is

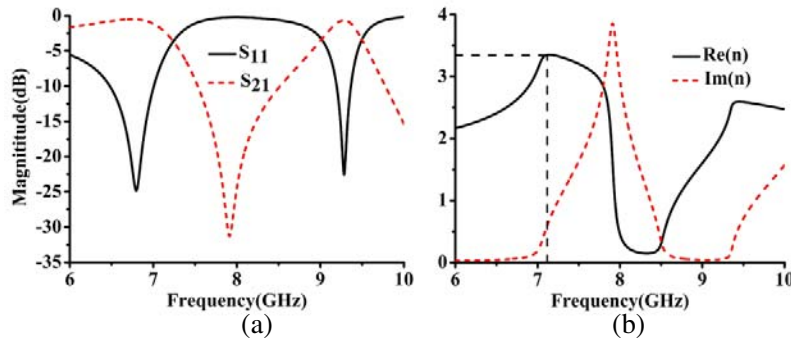


Figure 4. (a) The simulated S -parameters of the unit-cell. (b) The extracted refractive index of the HRIM.

designated at 7.2 GHz, which is below the magnetic resonance of the HRIM to enable EM energy to transmit through the HRIM.

The S parameters are then analyzed to extract the effective refractive index of the HRIM which is shown Fig. 4(b). We can see that when the dielectric substrate is loaded with the HRIM and the resonant frequency below the magnetic resonance, the refractive index is increased, and the magnitude of the refractive-index at 7.2 GHz is equal to the maximum of 3.4. When the dielectric substrate is loaded without the HRIM, the calculated refractive index of the pure dielectric substrate is 2.07. As a result, by applying the HRIM we have effectively increased the refractive index for a portion of the substrate. When the third harmonic of the dipole antenna is designated to be 7.2 GHz and the HRIM implemented in the broadside direction next to the CM before the dipole, the refractive index of the HRIM is larger than that of the dielectric substrate, and thus the two side lobes will be tilted toward the region with HRIM, namely the main beam radiation direction and the finalized radiation pattern are one main beam without side lobes and with higher directivity. Thus, gain enhancement can be obtained for the third harmonic resonance of the antenna.

4. SIMULATION AND MEASUREMENT RESULTS

To provide a verification of the side-lobe suppression method, two dipole antennas with and without the HRIM are fabricated and tested comparatively. The HRIM integrated on the dipole antenna is a 2×3 array of H-shaped metamaterial unit-cells. The simulated and measured reflection coefficients versus frequency are plotted in Fig. 5.

From Fig. 5, we can find that the dipole antenna without HRIM resonates at 2.4 GHz and 7.0 GHz, respectively, which corresponds to the fundamental and third harmonic resonances of the dipole antenna,

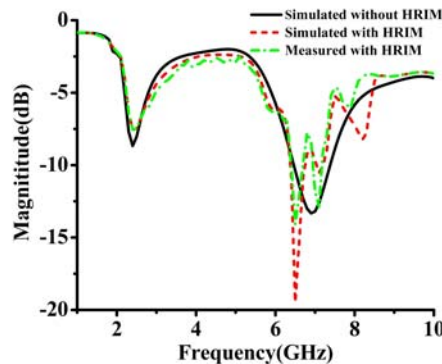


Figure 5. The simulated and measured reflection coefficients of the proposed antenna.

respectively. We can also observe that the integrated HRIM has non-negligible effect on the resonant frequencies of the antenna, because the HRIMs are electromagnetically coupled to the dipole arms, thus the resonances of the HRIM cannot be ignored. The dipole antenna with HRIM generally resonates at 6.3 GHz, 7.2 GHz, and 8.3 GHz, respectively. The resonances located at 6.3 GHz and 8.3 GHz correspond to the simulated two electric resonances of the HRIM unit cell, which are 6.8 GHz and 9.2 GHz, respectively. In this paper, the HRIM is finely designed at 7.2 GHz aiming at the third harmonic resonance for side lobe suppression purposes; therefore, only resonance at 7.2 GHz is taken into consideration. The simulated and measured results for the two prototypes are in good agreement except for slight discrepancy which may be caused by fabrication and installation errors.

To have a clear and straightforward view of the side-lobe suppression phenomenon, the simulated 3-D radiation patterns for both antenna prototypes are plotted in Fig. 6. From the picture we can clearly see that for the dipole antenna without HRIM, two side lobes beside the main beam in the broadside direction appear clearly at 7.0 GHz, which is caused by the current reversal, and the antenna gain is 5.5 dBi. However, when the dipole antenna is loaded with the HRIM, the two side lobes are suppressed at the third harmonic, and the antenna gain for the third harmonic is achieved as high as 7.8 dBi. As a comparison, the radiation patterns for both cases at 2.4 GHz remain unaffected, and only the antenna gain is increased from 3.3 dBi to 4.5 dBi because the antenna aperture is enlarged. As a result, the goal of suppressing the side lobe and keeping the radiation pattern consistent is achieved. Moreover, the antenna gain for the third harmonic is achieved as high as 7.8 dBi, which is an increase of approximately 3 dBi compared with the fundamental resonance. The fabricated prototypes are shown in Fig. 7, and the radiation patterns of the proposed antenna are measured in an anechoic chamber. The simulated and measured E -plane radiation patterns for both antenna prototypes are plotted. As can be seen in Fig. 8(a), for the traditional antenna, the main beam splits into two side lobes at $+240^\circ$ and $+120^\circ$, respectively, and the measured peak gain is a little lower than the simulated one for two side lobes. As can be seen in Fig. 8(b), the two side lobes have been suppressed a lot, and the main beam has appeared in the broadside direction, which denotes the $-x$ direction. The measured result agrees well with the simulated ones. Moreover, the measured antenna gain at 7.2 GHz reaches as high as 7.8 dBi, which is increased by 3 dBi compared with the fundamental resonance.

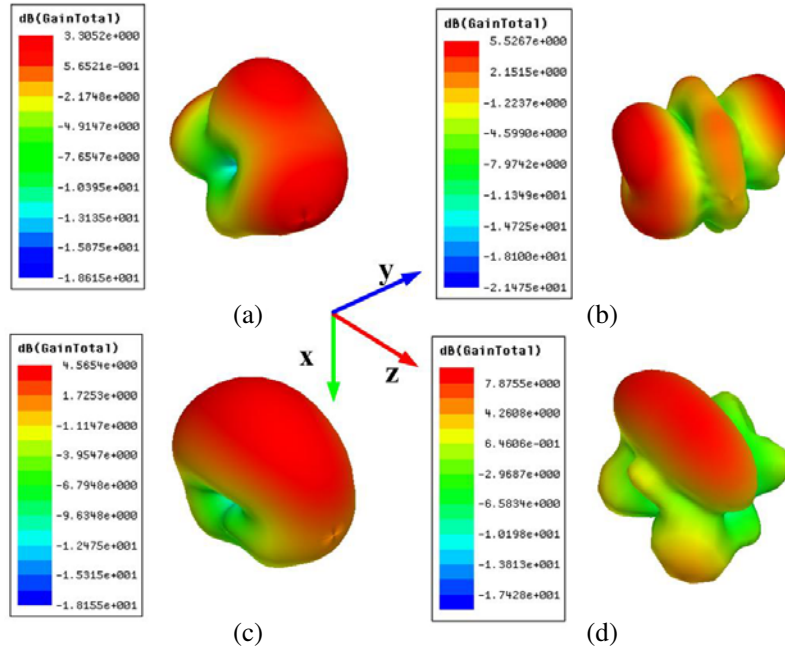


Figure 6. The simulated 3-D radiation patterns. (a) Conventional dipole antenna at 2.4 GHz. (b) Conventional dipole antenna at 7.0 GHz. (c) Dipole antenna loaded with HRIM at 2.4 GHz. (d) Dipole antenna loaded with HRIM at 7.2 GHz.



Figure 7. The photograph of the fabricated antenna.

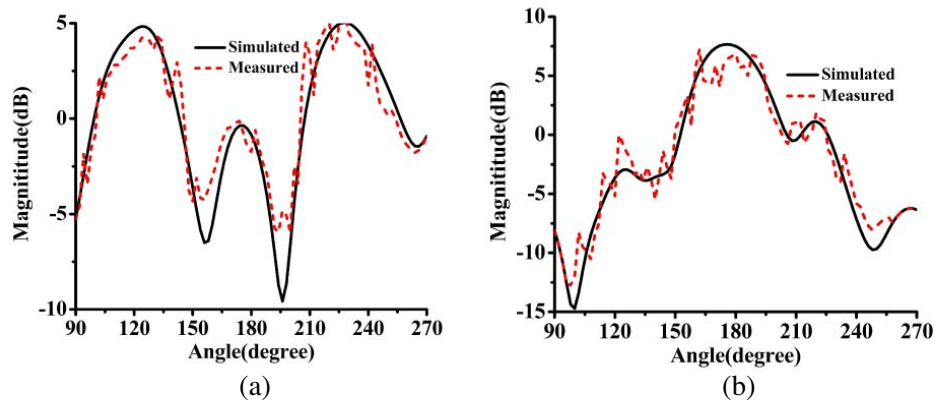


Figure 8. (a) Simulated and measured E -plane (XOY plane) radiation pattern for the traditional antenna without HRIM at 7.0 GHz. (b) Simulated and measured E -plane (XOY plane) radiation pattern for the antenna loaded with HRIM at 7.2 GHz.

5. CONCLUSION

In this paper, side-lobe suppression is realized successfully for the third harmonic resonance of planar dipole antennas by using HRIM. The high refractive index metamaterial is constructed with 2×3 H-shaped unit-cells periodically printed on the single side of dielectric substrates. The antenna prototype is a conventional planar dipole antenna backed by a metal reflector. Simulation and measurement results show that by implementing the HRIMs, the two side lobes are tilted toward the broadside radiation direction. As a result, side lobe is suppressed, and radiation consistency is realized. Moreover, the antenna gain for the third harmonic reaches as high as 7.8 dBi, an increment of approximately 3 dBi compared with the fundamental resonance, which means that we do not need an extra shorter dipole antenna to realize directional radiation patterns, and we can realize high gain antenna at the same time.

ACKNOWLEDGMENT

This work was supported by the National Natural Science Foundation of China under Grant 61372034.

REFERENCES

1. Balanis, C. A., *Advanced Engineering Electromagnetics*, Wiley, New York, NY, USA, 1989.
2. Laport, E. A. and H. Jasik, Editor, "Long-wire antennas," *Antenna Engineering Handbook*, 1st Edition, Chapter 4, 4-35, McGraw-Hill, New York, NY, USA, 1961.
3. Zhu, S. S., H. W. Liu, and P. Wen, "A new method for achieving miniaturization and gain enhancements of Vivaldi antenna based on anisotropic metasurfaces," *IEEE Trans. Antennas Propag.*, Vol. 10, No. 12, 102-135, Jan. 2019

4. Yang, Z. Q., L. M. Yang, and T. Yang, "A microstrip magnetic Yagi-uda antenna employing vertical I-shaped resonators as parasitic elements," *IEEE Trans. Antennas Propag.*, Vol. 60, No. 12, 5613–5626, Dec. 2018
5. Antoniadou, M. A. and G. V. Eleftheriades, "Multiband compact printed dipole antennas using NRI-TL metamaterial loading," *IEEE Trans. Antennas Propag.*, Vol. 60, No. 12, 5613–5626, Dec. 2012.
6. Li, D., Z. Szabó, X. Qing, E.-P. Li, and Z. Chen, "A high gain antenna with an optimized metamaterial inspired superstrate," *IEEE Trans. Antennas Propag.*, Vol. 60, No. 12, 6018–6023, Dec. 2012.
7. Jafargholi, A., M. Kamyam, and M. veysi, "Artificial magnetic conductor loaded monopole antenna," *IEEE Antennas Wireless Propag. Lett.*, Vol. 9, 211–214, 2010.
8. Wei, K., Z. J. Zhang, Z. H. Feng, and M. F. Iskander, "A Wideband MNG-TL dipole antenna with stable radiation patterns," *IEEE Trans. Antennas Propag.* Vol. 61, No. 5, 2418–2424, 2013.
9. Dadgarpour, A., B. Zarghooni, B. S. Virdee and T. A. Denidni, "Beam tilting antenna using integrated metamaterial loading," *IEEE Trans. Antennas Propag.* Vol. 62, No. 5, 2874–2879, 2014.
10. Chen, X., T. M. Grzegorzczuk, B. I. Wu, J. Pacheco, Jr., and J. A. Kong, "Robust method to retrieve the constitutive effective parameters of metamaterials," *Phys. Rev. Lett.*, Vol. E 70, p. 016608, 2004.
11. Qu, S.-W., J.-L. Li, Q. Xue, and C.-H. Chan, "Wideband periodic endfire antenna with bowtie dipoles," *IEEE Antennas Wireless Propag. Lett.*, Vol. 7, 314–317, 2008.